Biomedical & Translational Science

Original Article

Experimental Reconstruction of Critical Size Defects of Bone Tissue in the Maxillofacial Region When Using Modified Chitosan

Bolshakov Igor[1*], Levenets Anatoly[2], Furtsev Taras[3], Kotikov Alikhan[4], Patlataya Nadezhda[5], Ryaboshapko Ekaterina[6], Dmitrienko Anna[6], Nikolaenko Matvey[6], Matveeva Natalia[7] and Ibragimov Ilgizar[8]

[1]*Professor, Department Operative Surgery and Topographic Anatomy Professor V F Voyno-Yasenetsky Krasnoyarsk State Medical University, Russia*
[2]*Professor, Department Surgical Dentistry and Maxillofacial Surgery Professor V F Voyno-Yasenetsky Krasnoyarsk State Medical University, Russia*
[3]*Professor, Department Prosthetic Dentistry Professor V F Voyno-Yasenetsky Krasnoyarsk State Medical University, Russia*
[4]*Assistant Professor, Department Pathological Anatomy, Krasnoyarsk Clinical Regional Hospital, Russia*
[5]*Assistant, Department of Operative Surgery and Topographic Anatomy, Voronezh State Medical University named after N N Burdenko, Russia*
[6]*Dentistry Student, Professor V F Voyno-Yasenetsky Krasnoyarsk State Medical University Matveeva, Natalya, Russia*
[7]*Matveeva Natalia Dmitrievna - Medical Student, Professor V F Voyno-Yasenetsky Krasnoyarsk State Medical University Matveeva, Natalya, Russia*
[8]*FSBI National Medical Research Center named after EN Meshalkin, Russia*

Correspondence

Bolshakov Igor

Professor, Department Operative Surgery and Topographic Anatomy, Professor V.F. Vojno-Yasenetsky Krasnoyarsk State Medical University, Russia Address: Russia, Krasnoyarsk Territory, Krasnoyarsk, 660022 st. Partisan Zheleznyak, Russia

E-mail: bol.bol@mail.ru

Tel: +7 913 511 0933

- Received Date: 20 Feb 2022
- Accepted Date: 26 Feb 2022
- Publication Date: 01 Mar 2022

Keywords: critical size bone defect, nano-modified chitosan, atomic force microscopy, morphometry, CT-analysis

Abstract

Rationale: The authors of the article propose a biomaterial design based on highly deacetylated chitosan, which replaces extensive bone defects. In the work, a biomaterial was used included freeze-dried implants based on highly deacetylated and high molecular weight chitosan, containing natural polysaccharides and inorganic nano-structural hydroxyapatite by intervention in white laboratory rats.

Objectives: The goal is achieved due to the fact that a gel mass containing 2% chitosan ascorbate with a molecular weight of 100-700 kDa and a degree of deacetylation of 95-98% is introduced into large cavities. Sub-periosteal implantation of a chitosan structure into bone defects, CT analysis, morphometric analysis of histological sections of a bone defect allow us to reveal high efficiency in the early stages of bone reconstruction.

Findings: When using modified chitosan to fill extensive bone defects in the jawbone in animals, the process of defect replacement occurs after 4-5 weeks with the formation of a full-fledged new bone tissue compared to control animals. Morphological analysis of the bone defect on the 7th day after the intervention showed signs of cancellous bone tissue formation, two weeks later - a pronounced increase in bone tissue volume ($P < 0.01$). In the group with modified chitosan implantation, the amount of connective tissue formation was significantly lower ($P < 0.05$) compared to the control group. CT analysis showed that after 6 weeks after the intervention, the closure of the defect by 70-80% is recorded, after 8 weeks - complete 100% closure of the defect without disturbing the morphology of the bone with a high degree of mineralization.

Conclusions: Thus, modified chitosan is capable of eliminating bone defects of a critical size in the maxillofacial region, detecting early signs of angiogenesis and new bone formation, and serving as a promising material in reconstructive dentistry.

Introduction

Conformation of molecules and shape of chitosan nanoparticles. The role of pH in complexation

It should be noted that the efficiency of complexation of chitosan molecules with other compounds depends on the chitosan chain length, the charge ratio in the complex, and solvent properties, such as pH and ionic strength. The size of chitosan particles for a molecular weight of 1000 kDa is in the range of 48-52 nm, depending on the interpretation model of the conformational state of the molecular chain. The shape of a molecule in solution depends on pH: at pH <2, the molecule tends to the shape of a rigid rod, and at pH> 3, to the shape of a free coil. According to electron [1], the shape of chitosan nanoparticles and chitosan nano-complexes with other molecules is close to spherical. It is known [2] that in an acidic medium the chitosan molecule is converted into a polycation during the protonation of the amino groups -NH3+.

Citation: Igor B, Anatoly L, Taras F, et al. Experimental Reconstruction of Critical Size Defects of Bone Tissue in the Maxillofacial Region When Using Modified Chitosan. Biomed Transl Sci. 2022; 2(1):1-8

Consequently, the presence of charged particles in the immediate environment of chitosan is an effective factor in controlling the conformational state of the chitosan biopolymer.

Chitosan biopolymers in bone tissue reconstruction

Research in the field of bone tissue engineering using modern three-dimensional biodegradable matrices. Low mechanical strength, instability of maintaining the shape of the matrix base in native tissues limited the use of chitosan-based polysaccharide matrices for bone bioengineering [3-6], alginate [7-11], chondroitin sulfate [12], hyaluronic acid [13-14]. Improvement of the mechanical properties of these unique polymers has been achieved by the development of copolymers [15-20], also polyelectrolyte composites based on physical synthesis [21-23]. These properties were preserved when inorganic components are included in the matrix, for example, hydroxyapatites [24-26], protonated forms of chitosan, for example, with the help of weak organic acids, improve the functional properties of the hydrogel. In this case, the roughness of the surface of the matrix is also important: the nano-sized compared with the micro-sized surface is a stimulus for the proliferation of endothelial cells and osteogenic cells [27]. It is important to point out that the degree of deacetylation of the chitosan matrix plays an important role both in the timing of degradation of the structure and in the degree of endothelialization [28]. It has been established that constructions based on liquid polysaccharides, for example, the sulfated form of chitosan, chitosan ascorbate, chitosan hydrochloride, sodium salt of alginic acid, when introduced into the fascial sheaths of the neurovascular bundles [29] create the effect of therapeutic angiogenesis. The concept of the active inclusion of molecular markers of angiogenesis and further morphological restructuring of the qualitative and quantitative characteristics of the vessels consists in the artificial placement of chitosan and other biopolymers in the immediate affected area. Such a dislocation of polysaccharides leads to the normalization of not only the cellular and intercellular structure, but also to the macroscopic characteristics of the vessel, such as the thickness of the intima, media, the diameter of the main arteries, and the number of newly formed micro-vessels. In cases of bone regeneration, this concept of angiogenesis management may play an important role in the repair of giant defects in hard tissue. It should be noted that the size of chitosan nanoparticles significantly depends on the pH of the medium. On going from pH 1.55 to pH 3.5, the nanoparticle size decreases from 200-220 nm to 48-52 nm due to the pH-dependent change in the conformational state of the molecule. Most likely, in the environment of the stratified epithelium of the oral cavity, where the pH is close to 5.5, the chitosan particle size will clearly not exceed 50 nm. The nanometer scale of molecular sizes is a fundamental factor for the use of chitosan in medicine. In this job this compound contains chitosan of high purity and deacetylation, sodium chondroitin sulfate, sodium hyaluronate, heparin sulfate, sodium alginate, amorphous hydroxyapatite in certain weight ratios. The aim of the study is to increase the efficiency of restoration of full-fledged bone tissue in case of critical size defects of bone tissue with a microvascular bed in a shorter time after intervention. The goal is achieved due to the fact that a nano-gel mass Chitosan-Sodium Alginate-Hydroxyapatite (CS-SA-HA) is introduced into large cavities, These research is an example of experimental modeling of a real situation of protection of "small" molecules in aggressive media, for example, the oral cavity, and is directly related to solving the problem of targeted transportation of medicinal substances fixed on chitosan.

Materials and methods

Composition of Chitosan-Sodium Alginate-Hydroxyapatite (CS-SA-HA)

The Developer is SBEU HPT Krasnoyarsk State Medical University, Russia. Gel mass as part of CS-SA-HA containing a 2% solution of chitosan ascorbate (dissolution of the polymer in ascorbic solution acid in a ratio of 1: 1.5) with a molecular weight of 695 kDa and a degree of deacetylation of 95% (a triply purified chitosan obtained in Vostok-Bor-1, Dal'negorsk, Russia; Specifications (No 9289-067-004721224-97), including, per 1 g of dry chitosan ascorbate, 5-100 mg of sodium chondroitin sulfate (Sigma), 10-100 mg of sodium hyaluronate (Sigma), 2,5-5 mg of heparin sulfate (Russia, Pharm.Art. (No 42-1327-99), 110 mcg \ d serum growth factors in cattle "adgelon" (SLL "Endo-Pharm-A", Moscow region, Schcholkovo, Russia, Specifications (No 113910- 001-01897475-97), 4% sodium alginate (Pharm.Art. No 42-3383-97 or Specifications (No 15-544-83; Arkhangelsk algal plant. Co), including 50% amorphous hydroxyapatite (5-20 nm, Russia, Pharm.Art. (No 42-3790- 99 or GOST 12.1.007-76), in the ratio of chitosan ascorbate and sodium alginate 1:1. 7.2 grams of chitosan is added to the prepared solution of ascorbic acid (Pharm.Art. No 42-2668-95) with stirring at a temperature of + 20-25° C, the mass is stirred for 4-5 hours until the chitosan is completely dissolved. Aqueous solutions of sodium salts of chondroitin sulfuric acid, hyaluronic acid, and heparin are successively added to the resulting 4% chitosan solution with constant slow stirring using a magnetic stirrer in a total volume equal to the volume of chitosan ascorbate. The introduction of each subsequent ingredient is carried out only after homogeneous mixing of the previous one with the chitosan gel. As a result, a 2% chitosan poly-ionic complex is obtained. Next, a 4% aqueous solution (gel) of sodium alginate is prepared, 50% (by dry weight) of hydroxyapatite is added. The finished chitosan solution is thoroughly mixed with the sodium alginate solution using a high-speed mixer.

Control of the chitosan nanoparticles formation

The authors of the work used in the study highly deacetylated chitosan with a molecular weight of 660-695 kDa. It is known that the radius of gyration, which characterizes the average geometric size of a molecule, increases with an increase in molecular weight and in the range of molecular weights of the studied samples is from 24 to 99 nm. Knowing the length of the monomer unit of chitosan (0.5 nm) and its mass (160 g / mol), one can find the length of a chitosan molecule with a weight average molecular weight of 660 kDa in a linear conformation - about 2000nm. Consequently, in solution, chitosan molecules are in a folded chain conformation. Experiments to determine molecular weights and sizes in our work were performed for chitosan solutions of 0.457 wt% acetic acid at pH 4.2. The formation of a copolymer of chitosan with glycosaminoglycans is based on the physical interaction of the polymer amino groups with anionic molecules of sodium chondroitin sulfate, sodium hyaluronate, heparin sulfate at a certain concentration and pH solutions, the sequence inclusion of glycosaminoglycans into the gel medium of highly deacetylated chitosan. The data were obtained by atomic force microscopy and velocity sedimentation using a Multimode Nanoscope 3D atomic force microscope (Veeco, USA) and a disk centrifuge with an option for measuring particle size distribution (CPS Instruments, USA).

Experimental animals

The conditions of biological test systems in the CDI CI correspond to Guide for the Care and Use of Laboratory Animals, 8th edition, 2011, NRC, USA (Manual on the content and use of laboratory animals, 8th edition, 2011, national research Committee, USA). The content of animals in individually ventilated cells from poly-sulfone Sealsafe, 461×274×228 mm (production TECHNIPLAST.P. A.). The rooms, which contain biological test systems, controlled temperature (18-24 C), humidity (30-70%), illumination (12/12 h), the multiplicity of air (XII without recirculation). Control of climatic parameters is carried out in accordance with the SOP "control of climatic parameters in the premises of the vivarium." Distribution of feed and water is carried out at a fixed time, the change of litter is made once a week in accordance with the SOP "preparation of cells for biological test systems. Marking. Change of bedding, feed, water".

Modeling defects of the critical size of the mandibular angle in rats

The study was carried out on 90 female Wistar rats weighing 200 g. Laboratory animals were divided into 1 study (45 rats) and 1 control groups (45 rats). With strict selection of animals at all stages of the experiment, as well as during the preparation of histological material, in the end, 3-5 animals were used in the research results in each group: CT analysis (control - 45 individuals and experience - 45 individuals) - 5 animals per each observation period (3,5 days, 1,2,3,4,6,8 and 10 weeks); morphological analysis (control - 30 animals and experiment - 30 animals) 3-4 animals for each observation period. The exclusion from the results of morphological studies of some animals in all experimental groups is due to the insufficiently high quality of the histological section and the complexity of the morphometric analysis. The non-inclusion of a number of experimental animals with observation periods of 3.4 and 8 weeks in the study results indicates an insufficiently bright dynamics of bone tissue regeneration during morphological analysis. The final results of morphometric analysis included 20 control and 20 experimental animals: 3,5 days, 1,2 weeks - 3 animals each, 3,10 weeks - 4 animals each. In the study group, an extensive defect in the lower jaw was modeled with subsequent filling of the defect using the “CS-SA-HA” construction. In the control group, an identical bone defect was filled with a blood clot. Under general intramuscular anesthesia with Zoletil 100 at a dose of 3 mg / rat, the skin in the area of the lower jaw was treated with an alcohol solution of chlorhexidine, an incision was made on the lower jaw in the area of the alveolar ridge 1.5-2 cm long. Bluntly detached laterally m. masseter and periosteum, a rounded three-walled defect measuring 5 mm was applied on the alveolar ridge with a dental ball-shaped bur. During the work, the bone was “cooled” with boron with an aqueous solution of chlorhexidine. The cavity of the bone defect was drained with tampons and filled with a lyophilic mass "CS-SA-HA", the defect was closed with the periosteum, the skin was sutured with separate sutures with monofilament 5.0. The wound was treated with an alcohol solution of chlorhexidine. In order to prevent the development of the inflammatory process, the antibacterial drug ceftriaxone at a dose of 8 mg / rat, Within 3 days after the intervention, the animals received Tramadol anesthetic solution 0,2 mg 2 times daily. During the first 24 hours, animals were admitted to the water. Feeding was performed 24 hours after the intervention solely with a mixture of "Polyproten-nephro" (SLL "Protenpharma", Russia) for 3 days. Drug support was provided with a broad-spectrum antibiotic (ceftriaxone at a dose of 8 mg / rat). The stitches were removed on the 7th day after the intervention.

Morphological analysis of bone tissue

The mandibles of the animals were placed in a 10% solution of buffered formalin, then fragments of the bodies of the mandibles were separated in the area of the postoperative defect with the capture of unchanged bone along the perimeter for 5 mm and placed in the decalcifying solution "Trilon B" for a period of 24-48 hours. The decalcified fragments were dehydrated in increasing concentrations of isopropyl alcohol and were embedded in paraffin. On a MicroTec CUT4050 microtome, serial sections of 4-6 µm in thickness were made in the area of the bone defect in the direction of its outer and inner walls. Sections were stained with hematoxylin-eosin and picrofuchsin according to van Gieson. The finished preparations were analyzed using an Olympus BX45 microscope with an Olympus DP 25 attachment for photo-video documentation and the Cell ^ D software package at a magnification of x100, x200, x400. Evaluation of bone tissue repair was performed using the following histomorphometric criteria: volumetric density of bone and connective tissue, volumetric density of osteoid and vessels, number density of fibroblasts, segmented leukocytes, histiocytes, giant multinucleated cells, volumetric density of the implant. The numerical density of cellular structures was measured as the number of cells in relation to the area of the visual field at x400 magnification. The relative bulk density of the measured structures was determined by the formula: OOP (%) = (Sa / St) * 100, where Sa is the total area of all selected areas, St is the area of the digital image.

CT of bone defects

The study was carried out on a Ray Scan computerized cone-beam tomography (CBCT) (South Korea) with the following characteristics: 80 KVp, 6mA, 14 sec. Defects of the mandibular bone of laboratory rats in the region of the jaw body 5 mm in diameter were examined. Bone defects were filled with a blood clot - control 1 and a CS-SA-HA spongy structure - an experimental group of animals. X-ray assessment of the dynamics of bone regeneration was carried out 1 week, 2, 4, 6, 8, and 10 weeks after surgical trauma in the axial and sagittal planes with a slice thickness of 0.1 to 0,5 mm, which made it possible to evaluate both individual slices and the entire injury area (an arrow points to the area of the defect). Bone density was measured in housefields (HU)[30].

Statistical analysis

Statistical analysis applied to numeric morphometric data. Considering that morphometric data distribution was different from normal we applied nonparametric statistics. To estimate the difference between two independent groups we used Mann-Whitney U-test. The statistical analysis was performed in R software (version 4.0.2).

Results

To obtain chitosan nanoparticles with sizes that provide high permeability through cell membranes, various ingredients were added to chitosan - heparin, chondroitin sulfate, alginate, and hyaluronate. The mechanism of obtaining nanoparticles of chitosan using anionic additives, as well as the distribution of nanoparticles by size by the example of the interaction of chitosan with sodium chondroitin sulfate, heparin sulfate, sodium hyaluronate is presented by a chemical reaction: .

$$\left[R-NH_3^+\right]X^- + R^1-O-Na \rightarrow R-NH_2 + R^1-OH + X-Na \quad (1)$$

$$R-NH_2 + R^1-OH \leftrightarrow \left[R-NH_3^+\right]OR^{1-} \quad (2)$$

$\left[R-NH_3^+\right]X^-$ *chitosan salt*

R^1-O-Na *polysaccharide salts*

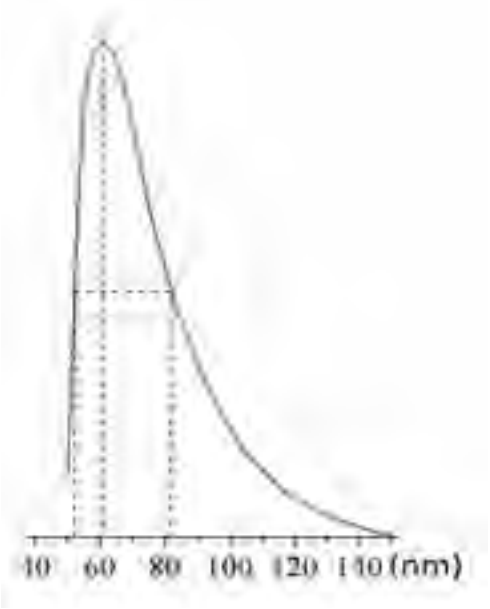

Figure 1. *Size distribution of polyelectrolyte complexes nanoparticles of chitosan with chondroitin sulfate*

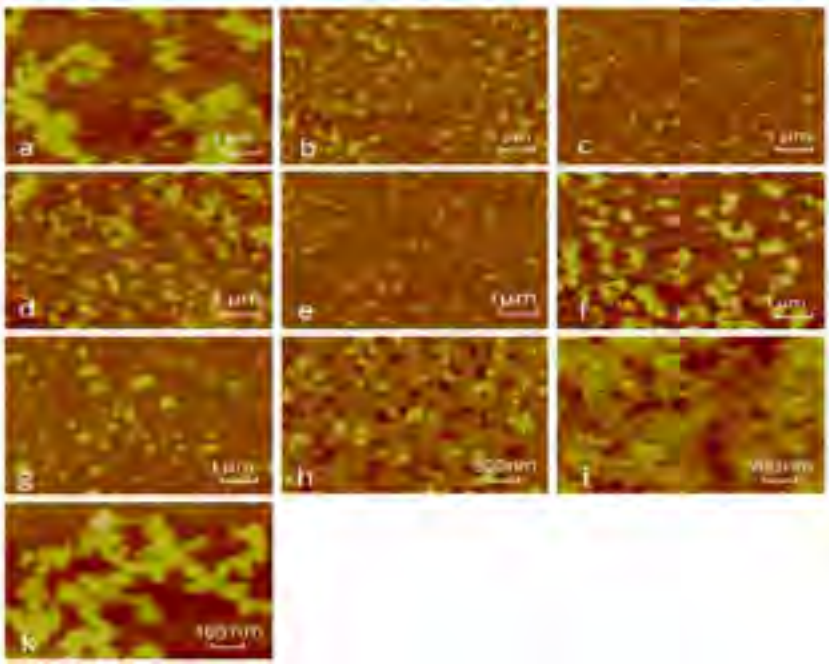

Figure 2. *Results of the study of the structure by atomic force microscopy at two magnifications: a) chitosan polycation (CS) has a partially folded chain conformation in acidic solution. Particle size depending on the type of additive: b) heparin sulfate (HS); c) chondroitin sulfate (CH); d) alginate sodium (SA). Change in concentration (for example, CH): e) 0,008%; f. 0,05%; g) 0,3%. Results of the study of bio-hydroxyapatite (Bio-HA) by atomic force microscopy; h-i). CS-SA-HA. Main components of the construction: chitosan ascorbate, sodium hyaluronate, heparin sulfate, chondroitin sulfate, sodium alginate, biohydroxyapatite (Bio-HA); k) results of the study of bio-hydroxyapatite (Bio-HA) by atomic force microscopy*

In the course of (1), amino groups of chitosan are formed, which as a result of (2) react with a free high molecular weight polybasic acid to form a salt of the polyelectrolyte complex. The increase in the molecular weight of the complex proceeds simultaneously with the structuring of the complex due to the electrostatic interaction of the ammonium centers of chitosan with the anionic centers of polysaccharides. As a result, of close electrostatic interaction, the particle size decreases, the degree of solvation decreases, and the insoluble phase of the substance appears in the form of nanoparticles. The size of the resulting nanoparticles depends on the structure and molecular weight of the starting polysaccharides, the ratio of the concentrations of chitosan and the anionic additive, as well as the degree of dissociation of the newly formed acids, which is maximum for heparin and chondroitin sulfonic acids. Analysis of the distribution of nanoparticles after mixing a 0.1 wt% chitosan ascorbate solution with a 0.05% chondroitin sulfate solution showed that the bulk of nanoparticles is located within 40-80 nm (Figure 1). The size of the nanoparticles is controlled by the method of light scattering during the technological process before the stage of filling the composite mixture into molds to obtain the finished product. The formation of chitosan nanoparticles in solutions containing anionic polysaccharide additives depends on a number of factors, the change of which makes it possible to obtain nanoparticles with given sizes and properties: the type of additives, the pH of the solution, the ratio of the concentrations of chitosan and molecular weight additives (Figure 2a-2k).

Morphological analysis of bone tissue restoration in the defect zone

Observational microscopy in the preparations of the defect area of the mandible of all the studied groups on the 3rd day after the operation determined the blood structure, a large number of inflammatory cells, among which segmented leukocytes predominated. In the preparations of the jaws, on the 5th day of observation, a predominance of immature connective tissue was noted in combination with a high number density of segmented leukocytes, fibroblasts, and histiocytes. In the preparations on the 7th day after intervention, signs of cancellous bone tissue formation were recorded in the area of the defect (Figure 3C), in some places in combination with cartilaginous tissue, the inflammatory reaction persisted, however, along with segmented leukocytes, rather numerous histiocytes were detected in the infiltrate. In preparations of 2 and 3 weeks in the area of the bone defect, the predominance of cancellous bone tissue and dense (mature) connective tissue was observed, scanty infiltrates were revealed, represented by histiocytes, lymphocytes and segmented leukocytes (Fiures 3D,3E). The area of the defect in the preparations of the mandible taken for analysis after 2.5 months of the experiment was characterized by a clear predominance of cancellous bone in combination with a poor connective tissue component (Figure 3F). The results of histo-morphometric studies are presented in Tables 1 and 2. As can be seen in the tables, graphs and photo-illustrations, the structures of the newly formed bone tissue were detected in the preparations already on the 7th day of the

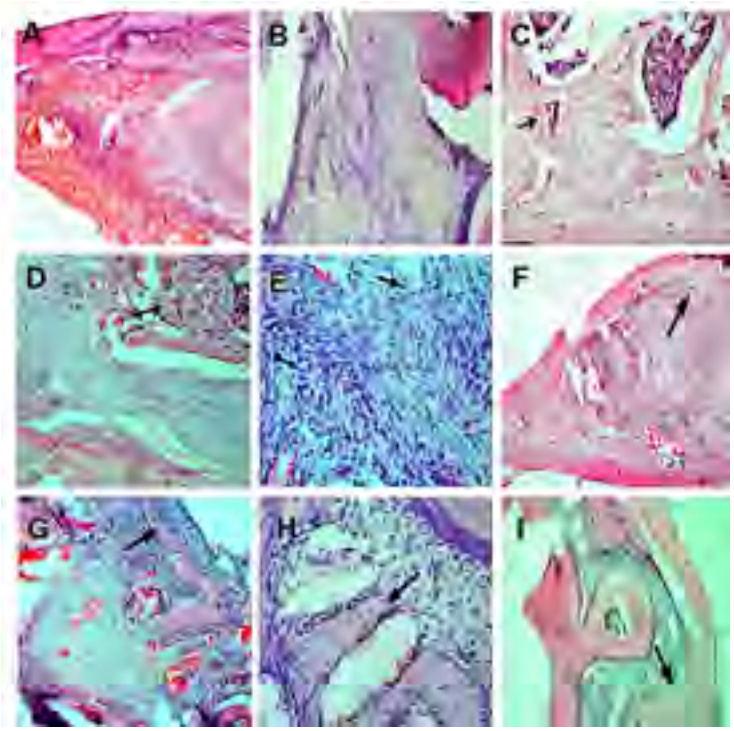

Figure 3. *Repair of the lower jaw defect at different times: A - under a blood clot (3 days; x40) - an extensive focus of hemorrhagic impregnation; B – under a blood clot (5 days; x40) – the bone defect is filled with granulation tissue; C – under a blood clot (7 days; x40) – a little island (arrow) of new forming bone tissue among granulation tissue; D – under a blood clot (2 weeks; x100) – an area of the forming bone (arrow) are revealed among the immature connective tissue; E - CS-SA-HA (5 days; x400) - granulation tissue with a high number density of polymorphonuclear leukocytes (arrow) and histiocytes (arrow with rectangle); F - CS-SA-HA (7 days; x40) – areas (arrow) of the forming bone are revealed among the immature connective tissue; G - CS-SA-HA (2 weeks; x100) - areas of regenerating bone (arrow) are identified among the elements of maturing connective tissue; H - CS-SA-HA (3 weeks; x200) - formed bone trabeculae (arrow) covered with osteoblasts; I - CS-SA-HA (2.5 months; x40) - formed bone tissue (arrow) along the periphery of the periodontium*

Table 1. *Histomorphometric data of bone tissue repair in mandibular size defect (principal components of bone tissue reparation and implant volume)*

Animals group	Bone volume	Connective tissue volume	Osteoid volume	Implant volume
Under a blood clot 3 days (n=3)	0	5.0 (3.5-5.2)	0	-
Under a blood clot 5 days (n=3)	0	35.6 (31.5-38.1)	0	-
Under a blood clot 7 days (n=3)	11.1 (9.3-12.2)	37.2 (34.5-39.1)*	1.05 (0.85-1.15)	-
Under a blood clot 2 weeks (n=3)	43.4 (39.3-47.1)*	33.3 (31.3-36.2)	1.7 (1.55-1.9)	-
Under a blood clot 3 weeks (n=4)	51.3 (45.5-56.5)	36.2 (29.5-37.2)	1.5 (1.35-1.7)	-
Under a blood clot 2.5 months (n=4)	75.2 (65.3-78.1)	5.2 (4.5-5.6)	0.7 (0.5-0.95)	-
CS-SA-HA 3 days (n=3)	0	4.3 (3.3-5.1)	0	35.4 (30.9-37.9)
CS-SA-HA 5 days (n=3)	0	34.6 (31.3-37.1)	0	33.7 (31.5-36.4)
CS-SA-HA 7 days (n=3)	12,2 (8.4-14.1)	32.2 (31.5-34.2)*	1.2 (1.05-1.3)	18.4 (15.2-21.1)
CS-SA-HA 2 weeks (n=3)	47.4 (45.5-49.2)*	31.8 (27.5-34.2)	1.4 (1.2-1.55)	12.2 (9.8-12.7)
CS-SA-HA 3 weeks (n=4)	48.6 (43.5-54.1)	36.2 (29.5-37.2)	1.1 (0.95-1.3)	14.2 (11.6-16.8)
CS-SA-HA 2.5 months (n=4)	73.2 (65.5-75.1)	4.9 (3.6-6.2)	0.2 (0.11-0.3)	5.3 (4.4-6.3)

Data presented as median (0.25-0.75);
* Significant level in comparisons with the same criterion of the compared group (P <0.05)

Table 2. *Histomorphometric data of bone tissue repair in mandibular size defect (cellular and vessel components)*

Animals group	Fibroblasts (Nx)	PMNL (Nx)	Histiocytes (Nx)	MGCs (Nx)	Vessel volume
Under a blood clot 3 days (n=3)	0	44.1 (41.9-47.2)	3.4 (2.1-3.9)	-	-
Under a blood clot 5 days (n=3)	25.3 (21.6-27.4)	49.6 (44.3-55.0)	11.2 (9.3-12.1)	-	5.1 (3.9-6.1)
Under a blood clot 7 days (n=3)	44.5 (42.1-47.3)	52.5 (47.1-54.3)	23.5 (20.1-25.4)	-	8.4 (7.9-9.7)
Under a blood clot 2 weeks (n=3)	39.0 (33.3-41.2)	19.5 (17.2-22.1)	11.4 (9.2-13.5)	5.5 (4.7-6.8)	4.2 (3.6-5.1)
Under a blood clot 3 weeks (n=4)	14.2 (11.9-16.1)	5.1 (4.1-6.3)	5.2 (4.5-6.5)	2.5 (1.9-3.4)	1.5 (0.8-2.3)
Under a blood clot 2.5 months (n=4)	8,5 (7.7-9.6)	2.1 (1.3-2.9)	6.1 (4.9-7.5)	2.0 (1.1-2.8)	0.85 (0.5-1.2)
CS-SA-HA 3 days (n=3)	0	41.2 (34.6-45.8)	4.1 (3.3-5.0)		
CS-SA-HA 5 days (n=3)	22.2 (19.2-24.3)	53.2 (48.2-56.7)	15.6 (13.1-17.3)		4.3 (3.4-5.5)
CS-SA-HA 7 days (n=3)	39.4 (31.8-43.3)	55.5 (49.2-59.1)	19.4 (16.5-21.1)		3.3 (2.6-4.3)
CS-SA-HA 2 weeks (n=3)	34,3 (28.4-37.3)	17.8 (13.2-21.1)	9.8 (7.7-10.7)	7.7 (6.4-8.2)	2.2 (1.7-2.9)
CS-SA-HA 3 weeks (n=4)	11,1 (9.9-12.8)	4.7 (3.7-5.5)	4.0 (3.2-5.3)	1.8 (1.4-2.2)	0.5 (0.4-0.6)
CS-SA-HA 2.5 months (n=4)	7.3 (6.6-8.3)	1.8 (1.5-2.1)	5.5 (4.3-6.3)	2.2 (1.8-2.5)	0.3 (0.2-0.4)

Data presented as median (0.25-0.75)
Nx – The number density; PMNL- polymorphonuclear leukocytes; MGCs- multinucleated giant cells;
* Significant level in comparisons with the same criterion of the compared group (P <0.05)

experiment (Figures 3c and 3F). In animals withdrawn from the experiment after the 2nd week, there was a pronounced increase in the volume of bone tissue (P <0.01) (Figures 3D and 3G). The volume of bone tissue in the group of animals in which CS-SA-HA was injected into the area of the bone defect was statistically higher after 2 weeks of the experiment in comparison with the volume density of bone tissue in the group without the use of biopolymers (P <0.05). It should be noted that after 3 weeks of the postoperative period, there were no significant differences between the groups represented. Analysis of the newly formed connective tissue in the area of the bone defect of the lower jaw in animals after 2 weeks of the experiment showed that in the group using CS-SA-HA this indicator was significantly lower (P <0.05) in comparison with the same indicator in the control group where bone repair was noted defect under the blood clot. Among other histo-morphometric parameters reflecting the reparation processes, one should highlight the high numerical density of segmented leukocytes in animals of the first week of the experiment (Figure 3F). This criterion, assessed in animals at a later date, has significantly lower values (P <0.001). Thus, on the basis of an objective histo-morphometric assessment, there are signs of a significantly higher dynamics of an increase in the volume of bone tissue at the early stages of the reparative process under conditions of using the CS-SA-HA preparation.

CT results of bone defect regeneration

In the control group, where the defect healed under a thrombus, the analysis showed that in the early stages from 3 days to 1 week after the injury, the dynamics of regeneration was absent. After 2 weeks, indistinct contours of bone regeneration are recorded. By the end of 3 weeks, the closure of the defect is observed by 30%, by the 4th week - by 50%, the bone tissue looks loose. After 6 weeks, the bone defect is closed by 80%, by the end of 8 weeks - by 90%. After 10 weeks, the bone defect closes 100%, while uniform healing is recorded without disturbing the morphology, the bone tissue is not dense enough, which for the cancellous part is 610-920 HU, compared to intact cancellous bone - HU 810-1012. When analyzing the density of bone tissue in the experimental group, X-ray signs confirm a higher density of the spongy substance, it is 810-1050 HU, and for the compact part of the bone - 1300-1500 HU, which is on average 18% higher than in the control. In the experimental group of experimental animals with filling of the bone defect with the CS-SA-HA construction, visual radiological changes were absent within 1 week after injury. 2 weeks after the application of a mechanical injury, the beginning of the regeneration of the bone defect is found in the form of fuzzy contours of the cavity facing the inside of the defect with islands of enlightenment. After 3 weeks, there is a positive trend in filling the defect with bone tissue in the form of "islands" of enlightenment. By the end of the 6th week, the closure of the defect by 70-80% with not yet mineralized bone tissue matrix is recorded, after 8 weeks there is a complete 100% closure of the defect without disturbing the bone morphology in the injury dislocation. By the end of the 10th weeks, complete closure of the defect with a higher degree of mineralization compared to the previous observation period. Bone density in HU units corresponds to a site of bone without injury. The CT data of bone defect regeneration are not entirely consistent with data of histological morphometric analysis of bone tissue. Particularly in the histological morphometric study we revealed the new bone formation in mandibular defect by first week, while the CT analysis detected the new bone formation only by second week. And furthermore, the volume of new bone formation according to CT was smaller by comparison with the same criteria estimated in histological morphometric analysis. This difference can be explained by low mineralization of new forming bone which prevents becoming adequate radio-opacity of the bone tissue. Decreasing this difference by the period of 2.5 month supports this approval. Thus, in the control, there is no complete restoration of bone mass, which is indicated by the presence of defects in the form of cavities.

Discussion

The addition of solutions of glycosaminoglycans (GAGs) in certain weight ratios and temperatures to a highly deacetylated chitosan gel with a high molecular weight forms nano-polyionic complexes capable of eliminating bone defects of a critical size in the maxillofacial region. Mixing chitosan sequentially with glycosaminoglycans leads to the formation of nanoparticles up to 100 nm in size, which is probably an important factor in rapid contact with the periodontal compartment. Morphometric and qualitative histological analysis of the lower jaw of rats showed that in the presence of a modified polyelectrolyte complex of chitosan, early signs of angiogenesis and the formation of new bone are recorded, starting from 7 days after the formation of a bone defect of critical dimensions. These are the results. Filling the vast operating bone cavity with CS-SA-HA material showed that by the end of the 4th week, the tomogram recorded the closure of the defect by 80%, and after 8 weeks - by 100%. 10 weeks after injury, there are no signs of a bone defect; the analysis registers dense bone corresponding to the density of healthy bone. These results are qualitatively different from previously published works, especially when analyzing the timing of the formation of a full-fledged bone in a large bone cavity. Thus, the idea of obtaining a nano-conjugate of highly deacetylated chitosan with glycosaminoglycans in order to form an active reaction of early angiogenesis and osteogenesis in the bone cavity of the critical size of the maxillofacial region probably significantly increases the impregnation of the polyelectrolyte polymer into the tissue compartment, significantly shortens the time for the formation of a full-fledged bone.

Summary

This work demonstrates the potential of polysaccharide biodegradable materials for the elimination of critical-sized bone defects in dentistry. Thus, thanks to the nano-size, one can expect to overcome the enzymatic or adsorption barrier, as well as an increase in the biotransformation of drugs. Therefore, the problem of optimizing the ratio of the surface area of a nanoparticle to its volume while maintaining the binding properties is urgent. Thus, according to the results of preliminary original studies of the structural, kinetic and adsorption properties of chitosan in solution and under conditions close to real in situ, scientific publications on the physics of nanoparticle formation and their properties obtained by other authors under similar conditions, the expected high transmembrane translation of growth factors and differentiation of osteoblast precursors in the finished product, early cell specialization in bone defects, and, ultimately, a high probability of bone tissue reconstruction, the authors proposed a technology for bone tissue restoration in the maxillofacial region with critical dimensions of postoperative defects. Obtaining such nano-sized products is a promising direction not only in maxillofacial surgery, but also in the field of dental transplantology, where it is required to create a tight contact between implants and bone.

Conflict of interest

The Authors declares that there is no conflict of interest.

Acknowledgments Annotation

The authors are grateful to the staff of the basic department of photonics and laser technologies of the Siberian Federal University for the analysis of the biotransformation of nanoparticles and chitosan molecules, a detailed interpretation of the physical processes during the formation of copolymers.

The work was carried out at each stage sequentially and consulted on the basis of the Center for collective use of scientific base Prof. V.F. Voyno-Yasenetsky Krasnoyarsk State Medical University and Federal Research Center "Krasnoyarsk Science Center of the Siberian Branch of the Russian Academy of Sciences" on the basis of contract No. 1-2 / 1 of 23/10/2017 and No. 1-2/2 of 23/10/2017. concluded between the Regional State Autonomous Institution "Krasnoyarsk Regional Innovative and Technological Business Incubator" ("KRITBI") and FSBEI HE Krasnoyarsk State Medical University named after prof. VF Voino-Yasenetsky of the Ministry of Health of the Russian Federation and trilateral agreement No. 2/t dated 09/13/2017 between KSAU "KRITBI", LLC "Bioimplant" (Krasnoyarsk) (General Director Bolshakov I.N.) and FSBEI HE KrasGMU named after prof. V.F. Voino-Yasenetsky. According to the trilateral agreement, the source of financing was KSAU "KRITBI", the source of co-financing of the project

was the limited liability company "Bioimplant" (Krasnoyarsk). The list of works included: chemical synthesis and production of variants of protein-polysaccharide gel; obtaining a solid product and the formation of oriented micro-channels for osteoblasts; modeling of extensive defects of the maxillofacial region in white rats, implantation of osteogenic matrices into bone defects; morphological analysis of bone tissue at various times after implantation in experimental animals; analysis of the physical and mechanical properties of the osteogenic matrix and bone tissue at various times after implantation; preparation of technological regulations for the production of osteogenic matrices.

References

1. Lakowicz JR. Principles of fluorescence spectroscopy. New York: Plenum.1999.
2. Zhang J, Yu BK, Wang CH. Holographic grating relaxation studies of camphorquinone diffusion in a polystyrene host. J Phys Chem. 1986; 90: 1299–1301.
3. Rodríguez-Vázquez M, Vega-Ruiz B, Ramos-Zúñiga R, Saldaña-Koppel DA, Quiñones-Olvera LF. Chitosan and its potential use as a scaffold for tissue engineering in regenerative medicine. BioMed Res Int. 2015; 821279.
4. Li Y, Kim JH, Choi EH, Han I. Promotion of osteogenic differentiation by non-thermal biocompatible plasma treated chitosan scaffold. Sci Rep. 2019;9(1):3712.
5. Costa-Pinto AR, Reis RL, Neves NM. Scaffolds based bone tissue engineering: the role of chitosan. Tissue Eng Part B Rev. 2011;17(5):331-347.
6. Costa-Pinto AR, Correlo VM, Sol PC, et al. Osteogenic differentiation of human bone marrow mesenchymal stem cells seeded on melt based chitosan scaffolds for bone tissue engineering applications. Biomacromolecules. 2009;10(8):2067-2073.
7. Gandhi JK, Opara EC, Brey EM. Alginate-based strategies for therapeutic vascularization. Ther Deliv. 2013;4(3):327-341.
8. Neufurth M, Wang X, Schröder HC, et al. Engineering a morphogenetically active hydrogel for bioprinting of bioartificial tissue derived from human osteoblast-like SaOS-2 cells. Biomaterials. 2014;35(31):8810-8819.
9. Nakaoka R, Hirano Y, Mooney DJ, Tsuchiya T, Matsuoka A. Study on the potential of RGD- and PHSRN-modified alginates as artificial extracellular matrices for engineering bone. J Artif Organs. 2013;16(3):284-293.
10. Saltz A, Kandalam U. Mesenchymal stem cells and alginate microcarriers for craniofacial bone tissue engineering: a review. J Biomed Mater Res A. 2016;104(5):1276-1284.
11. Venkatesan Ja, Nithya R, Sudha PN, Kim S-K. Role of alginate in bone tissue engineering. Adv Food Nutr Res. 2014;73(45):57.
12. Fan J, Park H, Lee MK, et al. Adipose-derived stem cells and BMP-2 delivery in chitosan-based 3D constructs to enhance bone regeneration in a rat mandibular defect model. Tissue Eng Part A. 2014;20(15-16):2169-2179.
13. Pandit AH, Mazumdar N, Ahmad S. Periodate oxidized hyaluronic acid-based hydrogel scaffolds for tissue engineering applications. Int J Biol Macromol. 2019;137:853-869.
14. Solchaga LA, Gao J, Dennis JE, et al. Treatment of osteochondral defects with autologous bone marrow in a hyaluronan-based delivery vehicle. Tissue Eng. 2002;8(2):333-347.
15. Chen S, Zhao XJ, Du C. Macroporous poly (L-lactic acid)/chitosan nanofibrous scaffolds through cloud point thermally induced phase separation for enhanced bone regeneration. Eur Polym J. 2018;109:303-316.
16. Munhoz MAS, Hirata HH, Plepis AMG, Martins VCA, Cunha MR. Use of collagen/chitosan sponges mineralized with hydroxyapatite for the repair of cranial defects in rats. Injury. 2018;49(12):2154-2160.
17. Carletti E., Motta A, Migliaresi C. Scaffolds for tissue engineering and 3D cell culture. Methods Mol Biol. 2011;695:17-39.
18. Jiang T, Khan Y, Nair LS, Abdel-Fattah WI, Laurencin CT. Functionalization of chitosan/poly(lactic acid-glycolic acid) sintered microsphere scaffolds via surface heparinization for bone tissue engineering. J Biomed Mater Res A. 2010;93(3):1193-1208.
19. Ouasti S, Donno R, Cellesi F, Sherratt MJ, Terenghi G, Tirelli N. Network connectivity, mechanical properties and cell adhesion for hyaluronic acid/PEG hydrogels. Biomaterials. 2011;32(27):6456-6470.
20. Moshaverinia A, Chen C, Xu X, et al. Bone regeneration potential of stem cells derived from periodontal ligament or gingival tissue sources encapsulated in RGD-modified alginate scaffold. Tissue Eng Part A. 2014;20(3-4):611-621.
21. Nejadnik MR, Yang X, Bongio M, et al. Self-healing hybrid nanocomposites consisting of bisphosphonated hyaluronan and calcium phosphate nanoparticles. Biomaterials. 2014;35(25):6918-6929.
22. Müller WE, Schröder HC, Feng Q, Schlossmacher U, Link T, Wang X. Development of a morphogenetically active scaffold for three-dimensional growth of bone cells: biosilica-alginate hydrogel for SaOS-2 cell cultivation. J Tissue Eng Regen Med. 2015;9(11):E39-50.
23. Sukpaita T., Chirachanchai S, Suwattanachai P, Everts V, Pimkhaokham A, Ampornaramveth RS. In vivo bone regeneration induced by a scaffold of chitosan/dicarboxylic acid seeded with human periodontal ligament cells. Int J Mol Sci. 2019;20(19):4883.
24. Chatzipetros E, Christopoulos P, Donta C, et al. Research application of nano-hydroxyapatite/chitosan scaffolds on rat calvarial critical-sized defects: a pilot study. Med Oral Patol Oral Cir Bucal. 2018;23(5):e625-632.
25. Hu JX, Ran JB, Chen S, Jiang P, Shen XY, Tong H. Carboxylated agarose (CA)-silk fibroin (SF) dual confluent matrices containing oriented hydroxyapatite (HA) crystals: biomimetic organic/inorganic composites for tibia repair. Biomacromolecules. 2016;17(7):2437-2447.
26. Luo Y, Lode A, Wu C, Chang J, Gelinsky M. Alginate/nanohydroxyapatite scaffolds with designed core/shell structures fabricated by 3D plotting and in situ mineralization for bone tissue engineering. ACS Appl Mater Interfaces. 2015;7(12):6541-6549.
27. Chung T-W, Liu D-Z, Wang S-Y, Wang S-S. Enhancement of the growth of human endothelial cells by surface roughness at nanometer scale. Biomaterials. 2003;24(25):4655-4661.
28. Amaral IF, Neiva I, da Silva FF, et al. Endothelialization of chitosan porous conduits via immobilization of a recombinant fibronectin fragment (rhFNIII(7-10)). Acta Biomaterialia. 2013;9(3):5643-5652.
29. Kirichenko AK, Patlataya NN, Sharkova AF, Pevnev AA, Kontorev KV, Bolshakov IN. Pathomorphism of limb major vessels in experimental atherogenic inflammation. The role of adventitial intimal relations (review). CTM. 2017;9(3):162-173.
30. Paukku P, Göthlin J, Tötterman S, Servomaa A, Hallikainen D. Radiation doses during panoramic zonography, linear tomography and plain film radiography of maxillo-facial skeleton. A comparative study. Eur J Radiol. 1983;3(3):239-241.